

Equilibrium Defect Concentration in Crystalline Sodium*

R. FEDER AND H. P. CHARBNAU

IBM Watson Research Center, Yorktown Heights, New York

(Received 12 April 1966)

The thermal expansion of high-purity sodium crystals has been measured from -25°C up to the melting point by precision interferometric and x-ray techniques. Above 15°C the two expansion curves diverge in a manner indicating a predominance of vacancy-type defects. The difference at the melting point is equivalent to a net vacancy concentration of 7.5×10^{-4} . Within experimental error, the divergence between the curves varies exponentially with reciprocal temperature and, if interpreted as due only to vacancies, yields a formation energy E_{1v}^f of 0.42 ± 0.03 eV and a formation entropy: $S_{1v}^f = (5.8 \pm 1.1)k$ (k is Boltzmann's constant). This value of E_{1v}^f accounts for almost all of the self-diffusion activation energy (0.45 ± 0.01 eV) and therefore leads to a very low value for the vacancy migration energy E_{1v}^m . Both the high value of S_{1v}^f and the low value of E_{1v}^m are consistent with the existence of a large lattice relaxation around a vacancy. Other possible interpretations of the results are also considered, involving the presence of divacancies or interstitials in addition to the monovacancies. However, the totality of evidence available from the present and other work favors the interpretation that monovacancies are the dominant defect in sodium both in the present measurement and in self-diffusion. Discrepancies between the present results and previous work have been attributed to the irreversibility in the macroscopic expansion caused by an oxide coating.

INTRODUCTION

MUCH work has been done in recent years in the area of point defects in metals. Most of this effort has however been confined to the noble or related face-centered-cubic (fcc) metals. Information on the energy and entropy parameters for the formation and motion of vacancies and divacancies in such metals has been reviewed recently by Seeger and Schumacher.¹ Comparable information for other classes of metals is either much less complete or nonexistent. This paper is concerned with a study of the point defects present in thermal equilibrium in the alkali metal sodium, which at normal temperatures and pressures exhibits the body-centered-cubic (bcc) crystal structure. Previous defect studies on sodium have given confusing results. For example, specific-heat² and resistivity measurements^{3,4} give values for the defect concentration at the melting point varying from 0.7 to 7.0×10^{-3} and for the formation energy varying from 0.2 to 0.39 eV.

The present investigation was undertaken to clarify the situation by the use of a more direct experimental method, which involves a comparison of the thermal-expansion curve of the lattice parameter with that of the bulk crystal over a large temperature range, extending almost to the melting point. The basis of this experiment is that these curves diverge from one another as a result of defect formation. The amount of divergence at any temperature is related to the equilibrium concentration of defects $\Delta N/N$ by

$$\Delta N/N = 3|\Delta l/l - \Delta a/a|, \quad (1)$$

* This work was partially supported by the U. S. Atomic Energy Commission.

¹ A. Seeger and D. Schumacher, in *Lattice Defects in Quenched Metals*, edited by R. M. J. Cotterill, M. Doyama, J. J. Jackson, and M. Meshii (Academic Press Inc., New York, 1965).

² L. G. Carpenter, *J. Chem. Phys.* **21**, 2244 (1953).

³ D. K. C. MacDonald, *J. Chem. Phys.* **21**, 177 (1953).

⁴ F. J. Bradshaw and S. Pearson, *Proc. Phys. Soc. (London)* **B69**, 441 (1956).

where $\Delta l/l$ and $\Delta a/a$ are the fractional changes in length and lattice parameter, respectively. The derivation of Eq. (1) is based on a theorem⁵ stemming from the work of Eshelby,⁶ which states that the lattice relaxation around a defect affects the linear expansion and the x-ray lattice-parameter expansion curve equally. As a consequence, the value of $\Delta N/N$ in Eq. (1) is determined only by the number of atoms either removed from or added to the surface of the crystal in forming the defects, Eq. (1) being a direct consequence. The value of $(\Delta l/l - \Delta a/a)$ can be positive or negative, according to the predominance of either vacancies or interstitials, respectively. If the observed value of $\Delta N/N$ at a temperature T is due to the presence of a single species of defect, $\Delta N/N$ is related to the energy (strictly enthalpy) and entropy of formation of the defect, E_d^f and S_d^f , respectively, by the equation

$$\Delta N/N = K \exp[-(E_d^f - TS_d^f)/kT], \quad (2)$$

where k is Boltzmann's constant and $K=1$ for a single vacancy or interstitial or is equal to the number of distinguishable orientations for defect pairs. The magnitude of S_d^f is controlled by the change in the lattice frequencies when a defect is introduced. This change becomes more positive as the frequencies decrease, i.e., S_d^f increases with greater relaxation of the lattice.⁷

With one exception, measurements of the type described above have been confined to fcc metals for which it is found that the simple vacancy is the dominant equilibrium defect.⁸ The energy for formation of a vacancy in fcc metals has so far always been found to account for approximately 50% of the activation energy for self-diffusion. The magnitude of the entropy

⁵ R. Feder and A. S. Nowick, *Phys. Rev.* **109**, 1959 (1958).

⁶ J. D. Eshelby, *J. Appl. Phys.* **25**, 255 (1954).

⁷ H. B. Huntington, G. A. Shirn, and E. S. Wajda, *Phys. Rev.* **99**, 1085 (1955).

⁸ R. O. Simmons and R. W. Balluffi, *Phys. Rev.* **129**, 1533 (1963).

factor appears to have a fairly constant value, with $S_{1v}^f/k \approx 1.5$.

The only previous investigation of point defects in a bcc metal by the x-ray-dilatometer expansion method appears to be that employed by Sullivan and Weymouth⁹ on sodium. The predominant defect was found to be the vacancy. The formation energy E_{1v}^f was estimated to be ≈ 0.14 eV, which is only one-third of the activation energy for self-diffusion ($Q=0.45$ eV) as measured by Nachtrieb, Catalano, and Weil.¹⁰

The results reported in this paper do not agree with those of Sullivan and Weymouth, and in addition presents some interesting contrasts with the behavior of fcc metals. The simplest interpretation of the present results is that (a) vacancies are greatly predominant over other thermal defects, (b) the vacancy-formation energy accounts for over 90% of the activation energy for self-diffusion, and (c) creation of a vacancy is accompanied by a large lattice relaxation, leading to a large value of S_{1v}^f . It will be shown that the only alternative to this is to postulate the coexistence of an appreciable number of interstitial atoms with the vacancies.

EXPERIMENTAL METHOD

Specimen Preparation

Single crystals of high-purity zone refined sodium were grown in an oil-coated stainless steel crucible using the Bridgman technique. The design of the crucible allowed the simultaneous crystal growth of a right-circular cylinder and a rod. The cylinder became the specimen for the dilatometer and the rod became the x-ray specimen.

The single-crystal rod was oriented on a goniometer table and made rigid by dipping the assembly in liquid paraffin. The rod was spark cut into 0.5-cm wafers with faces parallel to the (510) plane. The paraffin was dissolved in kerosene and two of the most perfect wafers were immersed in sodium-desiccated mineral oil. A thin (0.001-in.) disc of Mylar was placed on the front face of each wafer. Apiezon grease covered the remainder of one of the specimens. This treatment prevented any substantial discoloration for at least one hour, during which time the specimen was inserted into the x-ray camera and the camera evacuated. The nongreased wafer was exposed to the atmosphere for several hours so that the effect of the oxide on the lattice-constant expansion could be determined.

Each as-grown cylindrical sample of sodium was immersed in paraffin and spark cut to a length of 5.20 cm. The specimen was then placed in an argon-filled glove bag where the paraffin was removed and the specimen cleaned. A jig containing two optical flats

and a parallel right-circular steel cylinder was then used to compress the sodium specimen to a length of 5 cm, in order to produce flat and nearly parallel faces on the ends of the sample. This procedure was performed in an argon-filled glove bag attached to the dilatometer chamber, so that the atmosphere did not come in contact with the specimen. This manipulation technique proved to be very important, since other specimens which were transferred from the cleaning solution to the specimen chamber in air exhibited the undesirable dilatational hysteresis described below.

X-Ray Method

The equipment used to measure the lattice parameter is similar to that described by d'Heurle *et al.*¹¹ and Bond.¹² However, it was modified to operate at temperatures ranging from -25 to 600°C . A calibrated platinum-resistance thermometer was used to determine the specimen temperature. To obtain control at temperatures below room temperature, liquid nitrogen was passed through cooling coils wound alternately with the heating coils on the camera shell. Temperature gradients in the specimen and its mounting were minimized by the use of a helium atmosphere at a pressure of 100 Torr. The x-ray measurements were made on the (510) crystal plane, using Ni $K\alpha_1$ ($\lambda=1.65784$ Å) radiation. Over the temperature range from -25 to 98°C the corresponding Bragg angle varied from 82° to 78° , respectively. A double Mylar window was used on the x-ray camera as an entrance and exit port, to prevent frosting of the window during the low-temperature runs.

Dilatometer

Changes in length were measured using a Fizeau-type interferometer.¹³ In this system, the accuracy of the measured change in length is dependent only on the precision with which (a) the wavelength of the light source is known and (b) the shift in fringe pattern is determined. As shown in Fig. 1(A), the light beam is directed down the cylindrical specimen and is reflected from the bottom optical flat upon which the specimen rests. The incident and reflected beams interfere with each other on the lower face of the upper optical flat to produce the visible interference fringes. In this system an increase in the specimen length of $\frac{1}{2}\lambda$ causes a fringe shift of one complete fringe. It should be noted that the fringe shifts are dependent only upon the changes that occur in the specimen.

The two unique features in this equipment are the use of a He-Ne laser as the light source and the automatic fringe counting and recording system shown in Fig. 1(B). The entire assembly [Fig. 1(B)], consisting

⁹ G. A. Sullivan and J. W. Weymouth, *Phys. Rev.* **136**, A1141 (1964).

¹⁰ N. H. Nachtrieb, E. Catalano, and J. A. Weil, *J. Chem. Phys.* **20**, 1185 (1952).

¹¹ F. M. d'Heurle, R. Feder, and A. S. Nowick, *J. Phys. Soc. Japan* **18**, Suppl. II, 184 (1963).

¹² W. L. Bond, *Acta. Cryst.* **13**, 814 (1960).

¹³ See for example, R. W. Ditchburn, *Light* (Blackie and Son Ltd., London, 1952).

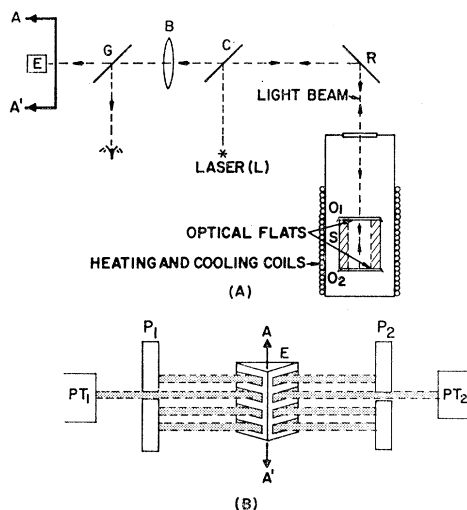


FIG. 1. Schematic diagrams of (A) side view of interference dilatometer and specimen chamber and (B) end view of fringe-counting system. O_1 , O_2 : optical flats, S : tubular specimen, R : silvered mirror, L : He-Ne laser, B : collimating lens, G : removable silvered mirror, E : silvered prism, P_1 , P_2 : slits, PT_1 , PT_2 : phototubes.

of a prism, two adjustable slits, and two phototubes, is first rotated so that the fringes are perpendicular to the apex of the prism E . Each fringe is then split into two parts with each phototube (PT_1, PT_2) seeing one-half of the incident fringes. Slits P_1 and P_2 are adjusted so that only one-half fringe is allowed to enter the phototubes at any time. By connecting the phototubes to a two-pen strip-chart recorder, the fringe shifts can be recorded as a series of sine waves. This double-recording system is employed because a single system may not detect a change in the direction of fringe movement. This condition can arise from an overshoot in temperature if the return to equilibrium occurs just as a fringe is leaving or entering the slit (crest or trough of the recorded sine wave). However, with the double system, if slit P_2 is adjusted so that the fringe

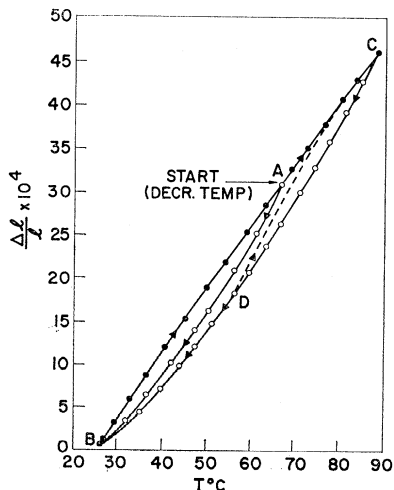


FIG. 2. Length expansion of sodium versus temperature, after exposure to the atmosphere for one hour. The irreversible curves were obtained by following the heating and cooling sequence $ABCBCDC$.

entering PT_2 is 90° out of phase with the fringe PT_1 , then at least one pen will reverse direction in an unambiguous manner, if the fringes reverse their movement. Subtraction of the number of fringes after such a reversal from the total number of recorded fringes gives the number of fringes due only to the specimen expansion between the initial and final temperatures. Temperature control of the specimen was obtained by immersing the tube containing the specimen into a closely regulated oil bath. A helium atmosphere at a pressure of 100 Torr was maintained in the specimen chamber to obtain good heat exchange. The temperature was read by means of a calibrated copper/constantan thermocouple placed about 2 mm from the outer surface of the specimen.

Precision of Measurements

To obtain an accuracy of about 1 part in 10^5 in measuring the differential between fractional change in lattice constant and the fractional change in length with temperature, the temperature of the two specimens was determined to better than $\pm 0.1^\circ\text{C}$. The x-ray and dilatometer specimens were found to maintain a gradient of less than 0.5°C and 0.1°C , respectively, when exposed to high temperatures (95°C). These gradients decreased with decreasing temperature. As a final check, to exclude the possibility of a systematic temperature error between the x-ray and length measurements, expansion measurements were made on an aluminum specimen from -25 to 120°C , over which range there is no reason to suspect a significant difference between x-ray- and linear-expansion behavior. All the lattice-parameter measurements were randomly scattered about the smooth dilatational-expansion curve, with the greatest deviation being accountable for by a temperature deviation no greater than 0.1°C .

In the interference dilatometer one fringe or sine wave represents a change in specimen length of $\frac{1}{2}\lambda = 3164.071 \times 10^{-8}$ cm for propagation in vacuo. By measuring to within 0.1 of a fringe, the corresponding error in the change in length ($\Delta l/l$) of a 5-cm specimen is 3.16×10^{-7} . For an atmosphere other than vacuum between the two optical flats, a small correction must be made to the wavelength noted above. This changes according to the Lorentz-Lorenz law; $(n-1) = (\text{const } \rho)$, where the index of refraction (n) depends upon the density (ρ) of the exchange gas being used.

RESULTS

It was discovered that, if a sodium specimen were exposed to the atmosphere for several minutes, the macroscopic expansion of the crystal becomes irreversible with temperature. Since the use of an expansion curve which is not a unique function of temperature can lead to erroneous conclusions, experiments were performed to ascertain the nature of the irreversibility and the conditions necessary to avoid its appearance. A plot

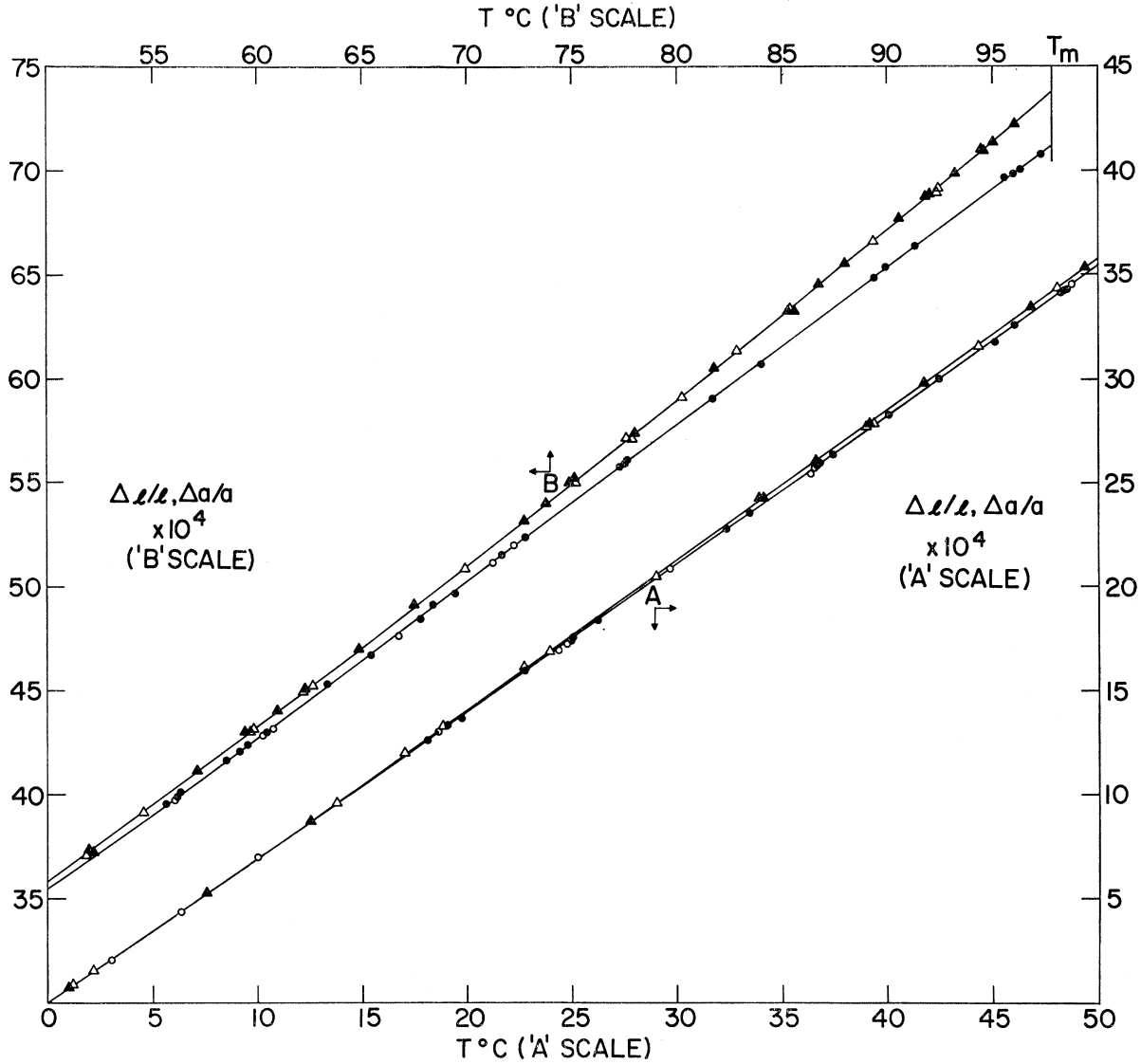


FIG. 3. Length and lattice-parameter expansion of sodium-versus-temperature. Curves A (0 to 50°C) are represented by lower and right-hand scales; curves B by left and upper scales. Circles represent lattice-parameter changes while triangles represent length changes. Open symbols are used for heating runs and filled symbols for cooling runs.

of $\Delta l/l$ as a function of temperature for several runs on an oxide-coated sodium specimen exposed to the atmosphere for one hour is shown in Fig. 2. The cooling and heating cycles follow the sequence *ABCBCDC*. Other experiments, using different initial temperatures and varying amounts of exposure to the atmosphere, confirmed that each heating and cooling run produced hysteresis of the type shown in Fig. 2, but of different magnitude. Figure 2 shows that as the temperature increases, the change in length increases, but at a decreasing rate. It was also observed that the fringes reversed their direction during the final slow approach to a higher constant value of the temperature, indicating an abnormal shrinkage of the specimen at a rate which outweighed the normal expansion. In a complementary

manner, when the temperature was decreased, the fringes reversed their direction before the temperature reached a lower constant value, indicating an abnormal specimen growth. Isothermal specimen shrinkage (following a heating step) and isothermal growth (following a cooling step) were observed for periods as long as 90 h to find out whether prolonged exposure to a constant temperature would eventually completely erase the hysteresis effect. Since this was found not to be the case, no unique relation exists between the length and the temperature of a specimen exposed to the atmosphere as described above. Later experiments linked this irreversible behavior with the presence of the oxide or hydroxide coating on the surface of the specimen. When the specimen was etched and kept in a dry

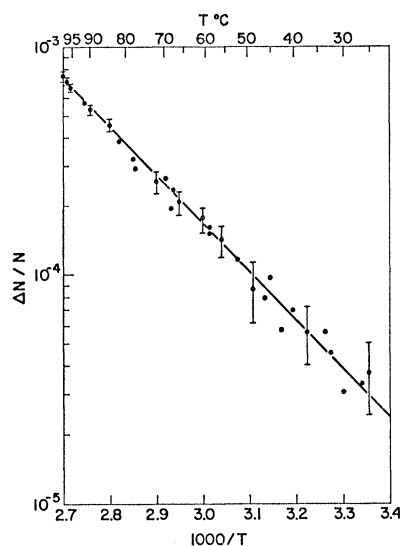


FIG. 4. Semilogarithmic plot of net-defect concentration versus reciprocal temperature. Bars represent average values of four or more lattice-constant measurements at designated temperatures.

argon atmosphere, the metallic surface changed to a pinkish color and complete dilatometric reversibility was obtained. However, upon re-exposure to the atmosphere the color of the specimen changed to white, with the subsequent appearance of the irreversibility. This process of removal of the skin and re-exposure was repeated several times and the effect was reproducible each time.

In contrast to the dilatational irreversibility described above, the lattice-parameter measurements made on companion crystals never exhibited irreversible or time-dependent effects, even when the specimens were coated with a white oxide skin.

The length measurements obtained from the non-exposed specimens are plotted in Fig. 3 as the fractional change in length ($\Delta l/l$) together with the fractional change in the lattice constant ($\Delta a/a$) as a function of temperature. The lattice constant and length measurements were made from -25 to $+97.4^\circ\text{C}$. The two expansion curves did not begin to diverge until 15°C . Consequently, for the sake of convenience the temperature scale in Fig. 3 starts from 0°C and the ordinate axis ($\Delta l/l, \Delta a/a$) is adjusted to zero at 0°C . The data points obtained from the length measurements represent results from runs on three specimens, whereas the x-ray data represents results from six specimens. Three of the x-ray specimens had received large exposures to the atmosphere. These specimens had thick white coatings before being placed in the x-ray camera. As remarked above, however, no difference was observed between the exposed and unexposed x-ray specimens. The solid symbols represent data points taken during heating runs and the open symbols represent data points obtained during cooling runs. The absolute value of the lattice parameter at 25°C was obtained by averaging over several specimens and found to be $4.28860 \pm 0.00012 \text{ \AA}$.

The maximum deviation of any individual experimental point from the smoothly drawn curves of $\Delta l/l$ and $\Delta a/a$ in Fig. 3 is 1×10^{-5} . The difference between the two curves at the melting point gives the positive value of 2.5×10^{-4} for $(\Delta l/l - \Delta a/a)$, so that, from Eq. (2), $\Delta N/N$ has the value 7.5×10^{-4} at the melting point. The data points representing the fractional change in lattice constant ($\Delta a/a$) do not fall at the same temperatures as the points for the fractional change in the length ($\Delta l/l$). Also, the precision of the $\Delta l/l$ curve is of a higher order than that of the $\Delta a/a$. Accordingly, all values of $\Delta N/N$ were obtained by taking the differences between the x-ray experimental points and the smooth curve for the macroscopic expansion. Figure 4 shows a logarithmic plot of $\Delta N/N$ as a function of the reciprocal temperature, obtained in this way. Often several x-ray measurements were made at the same temperatures, so that it was possible to obtain an average value for the $\Delta N/N$ at these temperatures. Whenever possible this averaging process was followed and the standard deviations calculated at such temperatures. The vertical bars represent the deviations of the experimental values about the mean. The remaining $\Delta N/N$ values are plotted as individual points. The solid line represents the best straight line through the mean values. Although a straight line is drawn through the data, a small positive curvature would also be consistent with the data. The maximum difference between any of the individual points and the smooth curve is less than 3×10^{-5} . The straight line in Fig. 4 is consistent with Eq. (2). We will define as the "effective" formation energy E' and entropy S' the values derived from the experimental slope and intercept of Fig. 4. Thus, only when a single defect species is involved will $E' = E_d'$ and $S' = S_d'$. The present data gives values of $0.42 \pm 0.03 \text{ eV}$ for E' and 5.8 ± 1.1 for S'/k .

DISCUSSION

Sullivan and Weymouth have reported results of a similar experiment on sodium. In describing their experiment they too remarked upon an anomalous behavior in the bulk-expansion measurements, whereby small irreversible increases in the length of their specimens occurred following thermal cycling. Because of this behavior they found they were able to obtain reproducible $\Delta l/l$ values only if the length measurements during heating cycles were used and if a correction were made for the initial length of the specimen prior to each heating cycle. It seems reasonable to assume that this irreversible behavior reported by Sullivan and Weymouth is the same as the hysteresis effect found in the present work. The continuous recording of the length changes by the interferometric dilatometer lends itself to a thorough examination of the shrinkage and growth processes of the sodium specimens. The results shown in Fig. 2, for example, represent the hysteresis obtained from a specimen exposed to the atmosphere

TABLE I. Comparison of present results with those previously reported.

	$10^4 \Delta N/N$ (mp)	E' (eV)	S'/k
Present work	7.5 ± 0.4	0.42 ± 0.03	5.8 ± 1.1
Sullivan <i>et al.</i> (mean value)	8.0 ± 1.4	0.14 ± 0.04	-3.2 ± 1.6

for a period of one hour, in which the surface exhibited a white coating and the specimen showed a change in length of 5 parts in 10^4 between the heating and cooling run. Sullivan and Weymouth reported that the surface of their specimens exhibited a dull metallic luster during their measurements and exhibited irreversible changes in length from 2 to 8 parts in 10^5 . Since the final results of the present experiment are only those on samples for which the irreversibility problem had been eliminated, it seems reasonable to attribute discrepancies with Sullivan's results to the hysteresis problem in the length measurements. In particular, their macroscopic expansion coefficient in the temperature region 0–97°C differs from the present experiment by 1 part in 10^{-4} .

A direct comparison between the two x-ray expansion coefficients between 0 and 97°C shows that the present results agree with one of Sullivan and Weymouth's samples to within 3 parts in 10^{-5} in $\Delta a/a$. This is within the combined experimental errors. Further comparisons can be made between the two experiments regarding the net-effective vacancy concentration found at the melting point and the effective energy of formation and entropy of formation of the defects. These comparisons are shown in Table I. The two values of the defect concentration ($\Delta N/N$) agree well within the experimental error. The large differences in the energy and entropy of formation are far beyond that which can be accounted for by experimental error. As already mentioned, it seems reasonable to explain the low values found by Sullivan *et al.* in terms of the irreversible behavior in the length measurements. For example, in Fig. 2 the $\Delta l/l$ curve representing the heating cycle (BAC) has negative curvature, whereas the true reversible $\Delta l/l$ curve shown in Fig. 3 has positive curvature. Because of this difference in curvature, the difference between the $\Delta l/l$ and $\Delta a/a$ curves for the sample subject to hysteresis will show depressed $\Delta N/N$ values at the higher temperatures and increased $\Delta N/N$ values at the lower temperatures. This results in an apparent low energy and entropy of formation.

We now turn to consider the significance of the present results. The fact that $\Delta l/l$ is greater than $\Delta a/a$ shows that the predominant defect in thermodynamic equilibrium at elevated temperatures is of the vacancy type. Further, the result of Fig. 4 shows that within experimental error, $\Delta N/N$ varies exponentially with $1/T$, which is consistent with the presence of a

single-defect species. We will see, however, that this conclusion is not the only possibility. Accordingly, the rest of the discussion is divided up into a consideration of the present results, first with the assumption that single vacancies alone are involved and secondly with the assumption that other defect species may coexist with single vacancies.

Case of Monovacancies Only

If single vacancies alone are involved in the present measurements, then the "effective" formation energy E' and entropy S' from the slope and intercept of Fig. 4, become the actual values for the formation energy and entropy of a single vacancy in sodium E_{1v}^f and S_{1v}^f , respectively. A formation energy of 0.42 eV is, in fact, in good agreement with the theoretical value obtained by Fumi,¹⁴ as well as the value obtained by MacDonald⁸ from the deviation from linearity of the resistivity of sodium at elevated temperatures.

If single vacancies are the only important defect in sodium and the present value of E' is their formation energy, then in the usual manner, it is possible to obtain the corresponding activation energy for migration by subtracting $E' = E_{1v}^f$ from the activation energy (Q) for self-diffusion. The most widely accepted value for the self-diffusion energy in sodium has been that reported by Nachtrieb *et al.*¹⁰ The more recent work by Barr and Mundy¹⁵ on the isotope effect in the self-diffusion of sodium confirm these results. The values of Q and the total entropy of activation S , obtained from the intercept D_0 , are listed in Table II in conjunction with the present values. The difference $Q - E_{1v}^f$ is then the activation energy for motion of a vacancy, or $E_{1v}^m = 0.03 \pm 0.03$ eV. This is a very unusual result, since E_{1v}^f accounts for 90% of the total activation energy Q , in striking contrast to the case of the fcc noble metals where the E_{1v}^f accounts for only about 50% of Q . The low value found for the migration energy in the present case also implies that it would be very difficult to attain a quenching speed necessary to retain an appreciable vacancy concentration. The only attempt of this kind was made by MacDonald,¹⁶

TABLE II. Best values for principal parameters.

		Ref.
Q (eV)	0.445 ± 0.005	10, 15
S/k	3.5 ± 0.7	10, 15
E' (eV)	0.42 ± 0.03	Present work
S'/k	5.8 ± 1.1	Present work

¹⁴ F. G. Fumi, *Phil. Mag.* **46**, 1007 (1955).

¹⁵ L. W. Barr and J. N. Mundy, in *Diffusion in Body Centered Cubic Metals* (American Society for Metals, Metals Park, Ohio, 1965).

¹⁶ D. K. C. MacDonald, in *Handbuch der Physik*, edited by S. Flügge (Springer-Verlag, Berlin, 1956), Vol. XIV, p. 137.

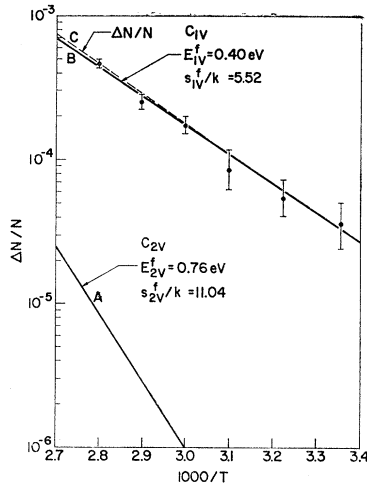


FIG. 5. Net concentration of monovacancies and divacancies versus $1000/T$ for particular choices of parameters. The dashed line represents the net defect concentration $\Delta N/N$ compared with the experimental values.

who was unable to retain a measurable vacancy concentration.

The present value of the entropy of formation is slightly larger than the total entropy, indicating a negative migrational entropy term where $S_{1v}^m/k = (S - S_{1v}^f)/k = -2.3 \pm 1.8$. The full meaning of a negative value for S_{1v}^m/k is not clearly understood at the present time.

The occurrence of a low value of E_{1v}^m and the high value of S_{1v}^f for the vacancy in sodium can both be rationalized if it is assumed that in the region surrounding the vacancy there is substantial relaxation. In the most extreme form, the region is described as liquid-like, with n atoms on $n+1$ sites, so that no particular site can be considered as occupied by the vacancy. This highly relaxed vacancy defect, sometimes referred to as the "relaxion", is a model which was first proposed by Nachtrieb and Handler,¹⁷ as a result of their work on the pressure dependence of self-diffusion. In addition to the present results, further support for such a model comes from the work of Barr and Mundy¹⁵ on the isotope effect in self-diffusion. These authors find a surprisingly small mass dependence of the self-diffusion coefficient. This can be interpreted, on the one hand, in terms of an interstitialcy mechanism, or on the other hand, in terms of the relaxed vacancy model. Since this work shows that the predominant defect is of the vacancy type, the former choice appears unlikely.

In summary, if we adopt the notion that only single vacancies are significant, we arrive at a value of E_{1v}^f which is about 90% of the Q for self-diffusion, and an unusually large value for S_{1v}^f . These results, although quite different from the fcc noble metals, are supported to some extent by theory,¹⁴ by resistivity and quenching experiments,^{2,16} and by the isotope effect in self-diffusion.¹⁵ On the other hand, we will see that this viewpoint does not represent the only possible interpretation of the present data.

¹⁷ N. H. Nachtrieb and G. S. Handler, Acta. Met. 2, 797 (1954).

Consideration of Other Defects

It is now worth considering the alternative possibility that the defect population is not made up of single vacancies only, but of monovacancies plus another type defect. The reason for introducing other defects is to see if there is an alternative explanation for the large values of the effective formation energy and entropy obtained in the present experiments. There are two types of defects which will be considered, the divacancy and the interstitial, each of which will be dealt with in turn. The following equations will be useful. The concentration of each type of defect in a bcc lattice is given by

monovacancy:

$$(\Delta N/N)_{1v} = C_{1v} = \exp(S_{1v}^f/k) \exp(-E_{1v}^f/kT); \quad (3)$$

divacancy:

$$(\Delta N/N)_{2v} = 2C_{2v} = 8 \exp(S_{2v}^f/k) \times \exp(-E_{2v}^f/kT); \quad (4)$$

interstitial:

$$(\Delta N/N)_i = C_i = \exp(S_i^f/k) \exp(-E_i^f/kT). \quad (5)$$

The binding energy and entropy (E_{2v}^b, S_{2v}^b) of a divacancy may be defined in the following manner:

$$E_{2v}^b = 2E_{1v}^f - E_{2v}^f, \quad (6)$$

$$S_{2v}^b = 2S_{1v}^f - S_{2v}^f. \quad (7)$$

The cumulative effect of the three types of defects under consideration in this type of experiment is

$$(\Delta N/N) = C_{1v} + 2C_{2v} - C_i. \quad (8)$$

To consider the possible role of divacancies, the binding energy (E_{2v}^b) is restricted to a value normally accepted for the fcc metals, of about 0.1 of the formation energy. Then E_{2v}^b for sodium is ≤ 0.04 eV. It is convenient to assume a binding entropy $S_{2v}^b = 0$. The values $E_{2v}^b = 0.04$ eV and $S_{2v}^b = 0$ should be regarded as those most favorable for divacancy production. A plot of $2C_{2v}$ is shown in Fig. 5 as curve A, while curve B for C_{1v} is deduced from Eq. (9) with $C_i = 0$ and $\Delta N/N$ made to fit the experimental curve as closely as possible. The resultant plot of $(\Delta N/N)$ is shown as the dashed curve and is seen to have a slight positive curvature. Error bars in this figure are redrawn from Fig. 4. This curve fits very well within the range of experimental results. The maximum number of vacancies associated as divacancies in Fig. 5 is $\sim 7\%$ of the total vacancy concentration. It is important to note, however, that the introduction of these divacancies has not made a significant difference in the values of E_{1v}^f and S_{1v}^f/k . The only way in which the fraction and importance of divacancies can be increased would be by increasing E_{2v}^b or making S_{2v}^b large and negative. At present there is no theoretical basis for

such choices, although Schottky *et al.*¹⁸ have argued that the entropy of binding in the noble metal fcc structures is negative. Even assuming a correspondingly large negative S_{2v}^b for the present case, the divacancy concentration could be brought up to 40% of the population, but the values of $E_{1v}^f = 0.39$ eV and $S_{1v}^f/k = 4.5$ obtained under these conditions are still quite high. It is therefore concluded that for reasonable values of E_{2v}^b and S_{2v}^b , the presence of divacancies would not do much to lower the values for E_{1v}^f and S_{1v}^f/k relative to those obtained by assuming that all defects present are single vacancies.

We now turn to a consideration of the possible role of interstitials. In this case the resultant defect concentration (shown in Fig. 4) must be made up of the difference between two exponentials (cf. Eq. (9) where $C_{2v} = 0$). In order for this analysis to be of value, it is necessary to impose certain conditions on the parameters making up the exponentials. First, the concentration of monovacancies C_{1v} must lie above the experimental curve in Fig. 4, since the total $\Delta N/N$ is positive. Second, values of E_{1v}^f and S_{1v}^f/k which are greater than the effective values (E^f and S^f) listed in Table II will not be considered since our objective is to see if the energy and entropy of formation of a monovacancy can be reduced to values more in line with those obtained in the fcc metals. Third, S_i^f should be ≤ 0 , since the presence of an interstitial should increase the vibrational frequencies.⁷ Fourth, the difference between the C_{1v} and C_i curves should lie within the error bars of Fig. 4 to be consistent with the present experimental results.

Assigning various values to E_{1v}^f and S_{1v}^f/k , several combinations of values of E_i^f and S_i^f/k were found which meet the above conditions. These energy and entropy values give rise to interstitial concentrations at the melting point ranging from 0 to 32%. As an example, the curves for the case of highest interstitial concentration and the corresponding vacancy concentration are shown in Fig. 6. It should be noted that this condition produces a curvature in the $\Delta N/N$ curve which is negative, to a point which may be regarded as almost outside of experimental error (compare Fig. 4). The corresponding energy and entropy values are

$$\begin{aligned} E_{1v}^f &= 0.28 \text{ eV} & E_i^f &= 0.20 \text{ eV} \\ S_{1v}^f/k &= 2.0 & S_i^f/k &= -1.0. \end{aligned}$$

The above values for the monovacancy defect are similar to the values found for the fcc metals, since E_v^f is only 60% of the total activation energy and the entropy of formation of a vacancy is close to previously

¹⁸ G. Schottky, A. Seeger, and G. Schmid, *Phys. Status Solidi* **4**, 439 (1964). This paper suggests that S_{2v}^b has a large negative value for the fcc noble metals. The validity of this argument in the case of the alkali metals is highly questionable.

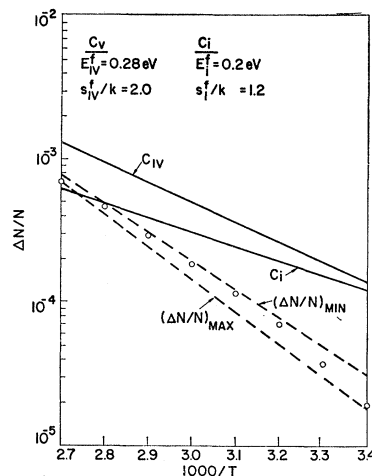


FIG. 6. Concentration of monovacancies and interstitials versus $1000/T$ for particular choices of parameters. The dashed lines represent maximum and minimum slopes of measured $\Delta N/N$ curve. Circles represent the calculated net-defect concentration.

reported values. With these numbers, plus the expectation that $E_i^m < E_{1v}^m$, it might then appear that self-diffusion should be attributable to interstitials, particularly at lower temperatures. There is strong evidence for rejecting the possibility that interstitials are predominant in self-diffusion. First, the effect of pressure on the self-diffusion in sodium reported by Nachtrieb *et al.*¹⁹ shows that the rate of self-diffusion decreased with an increase in pressure, i.e., that the activation volume is positive and equal to about half the atomic volume. It seems difficult to reconcile this result with an interstitial mechanism. Second, the plots of $\ln D$ versus $1/T$ obtained by both Barr *et al.* and Nachtrieb *et al.* show no curvature and therefore indicate that there is only one defect controlling diffusion. For example, Fig. 6 suggests that $C_{1v} \gg C_i$ at the melting point, but that $C_{1v} = C_i$ at about 30°C. The diffusion coefficients are measured down to 0°C and give no indication of a change in the diffusion mechanism. It is concluded, therefore, that although interstitials may be present to a small extent, the totality of evidence, both from diffusion and the present experiments makes it difficult to believe that their presence can substantially alter the conclusion that the measured values of E^f and S^f are, respectively, equal to E_{1v}^f and S_{1v}^f . Accordingly, the model of the highly relaxed vacancy seems best to describe the dominant defect in sodium.

ACKNOWLEDGMENTS

The authors wish to thank Dr. A. S. Nowick and Dr. B. S. Berry for many valuable and stimulating discussions on this work, and to K. Asai for his help in designing the dilatometer. The authors are also indebted to Dr. D. Lazarus and Dr. F. G. Fumi for their helpful comments on this manuscript.

¹⁹ N. H. Nachtrieb, J. A. Weil, E. Catalano, and A. W. Lawson, *J. Chem. Phys.* **20**, 1189 (1952).